Millennial-Scale Precipitation Variability in the Indo-Pacific Region Over the Last 40 Kyr

Zhaojie Yu, Xiaojie Tang, Christophe Colin, David J Wilson, Xinquan Zhou, Lina Song, Fengming Chang, Shuai Zhang, Franck Bassinot, Shiming Wan

Geophysical Research Letters

RESEARCH LETTER
10.1029/2022GL101646

Millennial-Scale Precipitation Variability in the Indo-Pacific Region Over the Last 40 Kyr

Zhaojie Yu[1,2,3], Xiaojie Tang[1,4], Christophe Colin[5], David J. Wilson[6], Xinquan Zhou[7], Lina Song[1], Fengming Chang[1], Shuai Zhang[8], Franck Bassinot[9], and Shiming Wan[1]

[1]Institute of Oceanology, Chinese Academy of Sciences, Qingdao, China, [2]Laboratory for Marine Geology, Pilot National Laboratory for Marine Science and Technology, Qingdao, China, [3]Center for Ocean Mega-Science, Chinese Academy of Sciences, Qingdao, China, [4]University of Chinese Academy of Sciences, Beijing, China, [5]Université Paris-Saclay, CNRS, GEOPS, Orsay, France, [6]Department of Earth Sciences, University College London, London, UK, [7]State Key Laboratory of Marine Geology, Tongji University, Shanghai, China, [8]College of Oceanography, Hohai University, Nanjing, China, [9]LSCE/IPSL, CEA-CNRS-UVSQ, Université Paris-Saclay, Gif-sur-Yvette, France

Abstract Deep atmospheric convection in the Indo-Pacific Warm Pool (IPWP) represents a major source of heat and moisture, thereby affecting the global climate, but its past changes remain debated. Here, we present sub-millennial clay mineralogy and elemental records spanning the last 40 Kyr from within the IPWP. From these data, we infer millennial-scale fluctuations in precipitation, with generally lower precipitation during Heinrich Stadials 1–4, corresponding to El Niño-like conditions. Higher precipitation coincided with the warm interstadials, accompanied by La Niña-like conditions. Moreover, our record indicates the lowest precipitation occurred during the late Holocene, supporting the hypothesis of a stronger-than-modern Walker circulation during the Last Glacial Maximum. In combination with other proxy records and TraCE-21 modeling results, we recognize a distinct spatial heterogeneity of precipitation within the IPWP, resulting from the dominant influences of the ENSO-like system and migration of the Intertropical Convergence Zone in the eastern and western IPWP, respectively.

Plain Language Summary Tropical rainfall systems in the Indo-Pacific Warm Pool (IPWP) play a significant role in transferring energy and moisture. However, their millennial-scale variabilities in precipitation during the past remain poorly understood. Here, we provide sub-millennial sediment mineralogy and elemental reconstructions spanning the last 40,000 years from a sediment core in the IPWP. We infer that variability in precipitation induced by atmospheric convection in the IPWP is the main factor controlling the variability in our data through time. Hence, we interpret our records to reflect millennial-scale fluctuations in precipitation, with lower precipitation during cool stadial periods and higher precipitation during warm interstadials. Such variability corresponds to the changing zonal state of the tropical Pacific atmosphere-ocean system, in a pattern similar to the modern-day. Additionally, our record indicates that precipitation was weaker during the late Holocene than during the Last Glacial Maximum (LGM), suggesting that the Pacific atmospheric zonal circulation was stronger during the LGM than today. Furthermore, a model-data comparison reveals distinct spatial heterogeneity in the precipitation changes, with precipitation in the eastern IPWP (West Pacific) likely controlled mostly by the tropical Pacific atmosphere-ocean system, whereas precipitation in the western IPWP (Indian Ocean) was driven by latitudinal movement of the Intertropical Convergence Zone.

Key Points:

- We present sub-millennial clay mineral and elemental records from the Indo-Pacific Warm Pool spanning the last 40 Kyr
- Our records indicate higher precipitation during La Niña-like conditions and lower precipitation during El Niño-like conditions
- Different patterns and controls on precipitation variability between the eastern and western Indo-Pacific regions are revealed

Supporting Information:

Supporting Information may be found in the online version of this article.

Correspondence to:

Z. Yu,
yuzhaojie@qdio.ac.cn

Citation:

Yu, Z., Tang, X., Colin, C., Wilson, D. J., Zhou, X., Song, L., et al. (2023). Millennial-scale precipitation variability in the Indo-Pacific region over the last 40 Kyr. *Geophysical Research Letters*, *50*, e2022GL101646. https://doi.org/10.1029/2022GL101646

Received 8 OCT 2022
Accepted 1 DEC 2022

1. Introduction

The Indo-Pacific Warm Pool (IPWP) is not only a major source of heat and moisture, but its deep atmospheric convection is also a key factor that affects the Walker and Hadley circulations (Sardeshmukh & Hoskins, 1988). However, the nature of past changes in deep convection since the Last Glacial Maximum (LGM), and the associated millennial-scale precipitation changes, remain unclear (Leduc et al., 2009; Mohtadi et al., 2017), largely due to the complex interactions between multiple climatic drivers and discrepancies between different paleo-precipitation indicators. It is hypothesized that the meridional migration of the Intertropical Convergence Zone (ITCZ) (Denniston et al., 2013; Griffiths et al., 2009; Huang et al., 2020; Krause et al., 2019; Kuhnt et al., 2015; Mohtadi et al., 2011, 2014; Partin et al., 2007; Schneider et al., 2014; Schröder et al., 2018; Wurtzel et al., 2018; Zhang & Delworth, 2005), variability of the El Niño-Southern Oscillation (ENSO) system (Liu et al., 2014; Timmermann et al., 2005; Turney et al., 2004), and changes in the Australian Monsoon strength

(Ayliffe et al., 2013; Denniston et al., 2013; Griffiths et al., 2009; Leduc et al., 2009; Mohtadi et al., 2011, 2016; Zhang & Delworth, 2005) could all respond to North Atlantic millennial-scale climate oscillations, and thereby affect precipitation in the Indo-Pacific region, but their relative importance is not well constrained.

A compilation of millennial-scale deglacial precipitation reconstructions from the IPWP region reveals a "seesaw" precipitation pattern in the western part (Indian Ocean) that could be explained by a meridional migration of the ITCZ (i.e., inverse precipitation patterns between regions A and B; Figures 1a and 1b). In contrast, precipitation in the eastern part (West Pacific) displays a "sandwich-like" pattern in the modern day (i.e., intrusion of region C, with areas to both the west and east belonging to region A; Figure 1a) and spatial heterogeneity in precipitation through the last deglaciation (Figure 1c). Such an east/west discrepancy and the "sandwich-like" precipitation pattern in the east cannot simply be explained by ITCZ migration, and may instead reflect an influence of the ENSO-like system, but that suggestion needs further verification (Xiong et al., 2018).

Most proxy records of precipitation in this region, which can be taken as an approximate indicator of IPWP convective intensity, are based on water isotopes or element ratios from XRF-scanning of sediment cores, both of which have limitations. For example, XRF-scan element ratios generally represent the relative change in sediment input from terrestrial sources versus marine productivity (e.g., K/Ca, Ti/Ca), such that other elemental ratios that are largely independent of marine productivity variations (e.g., K/Ti, Rb/Zr) may be required to exclude productivity influences (Fraser et al., 2014; Xiong et al., 2018). In addition, sea-level change may have an important impact on both element-based and water isotope-based proxies in the IPWP, mainly through changing the land-sea configuration or the distance and mode of sediment/moisture transport to a site (Carolin et al., 2016; Liu et al., 2009). Hence, indicators that are unaffected (or less affected) by such complicating factors would be complementary to existing records from water isotopes and XRF-scanning, and could provide independent constraints to verify the evolution of tropical precipitation in response to regional ocean-atmosphere processes.

Here, we present high-resolution records of clay mineralogy and element ratios spanning the last 40 Kyr from marine sediment core MD01-2385 (Figure 1), with average mineralogical and elemental sample spacing of ~75 and ~400 years. These terrigenous weathering records provide independent evidence constraining tropical precipitation changes in Northwest New Guinea. In combination with our compilation of paleo-records from the IPWP based on water isotopes and XRF-scanning, and TraCE-21 modeling results, we demonstrate a spatially heterogeneous pattern of millennial-scale precipitation variability in the Indo-Pacific region. Leduc et al. (2009) suggested that the migration of the ITCZ plays an important role in driving precipitation changes in this region on a large spatial scale (i.e., IPWP vs. northern Australia). Our study complements that work by demonstrating the significance of the ENSO-like system for driving millennial-scale precipitation changes, and helps to resolve the spatial extent of the ITCZ and ENSO-like influences on precipitation within the IPWP. Our results could therefore help to improve our understanding of future atmospheric patterns and precipitation changes in this region.

2. Regional Setting

During the boreal summer from June to July, southeast winds are dominant and the precipitation in the study area is ~400 mm/month (Figures S1b and S1c in Supporting Information S1), while the ITCZ takes a northern position over Northwest New Guinea. In contrast, during the boreal winter from January to February, the dominant wind direction changes to northwesterly, and the precipitation is reduced to ~200 mm/month (Figures S1a and S1c in Supporting Information S1), with a southward shift of the ITCZ. On inter-annual timescales since 1980, the monthly precipitation anomaly over the study area is highly consistent with the Southern Oscillation Index and the Niño 3.4 sea surface temperature (SST) anomalies (Figure S1d in Supporting Information S1), both of which represent the intensity of the Walker circulation and ENSO state. Therefore, there is co-variability between the zonal Pacific SST gradient, ENSO state, and the precipitation intensity in our study area. Specifically, a higher zonal Pacific SST gradient, and the associated stronger atmospheric pressure gradient, enhances the Pacific Walker circulation, leading to La Niña conditions that maintain the deep atmospheric convection center and higher precipitation over the tropical western Pacific (Figure S1d in Supporting Information S1). In contrast, a weaker zonal Pacific SST gradient is associated with El Niño conditions, a weakened Pacific Walker circulation, and an eastward shift of the deep convection and precipitation center, leading to reduced precipitation in the tropical western Pacific (Figure S1d in Supporting Information S1).

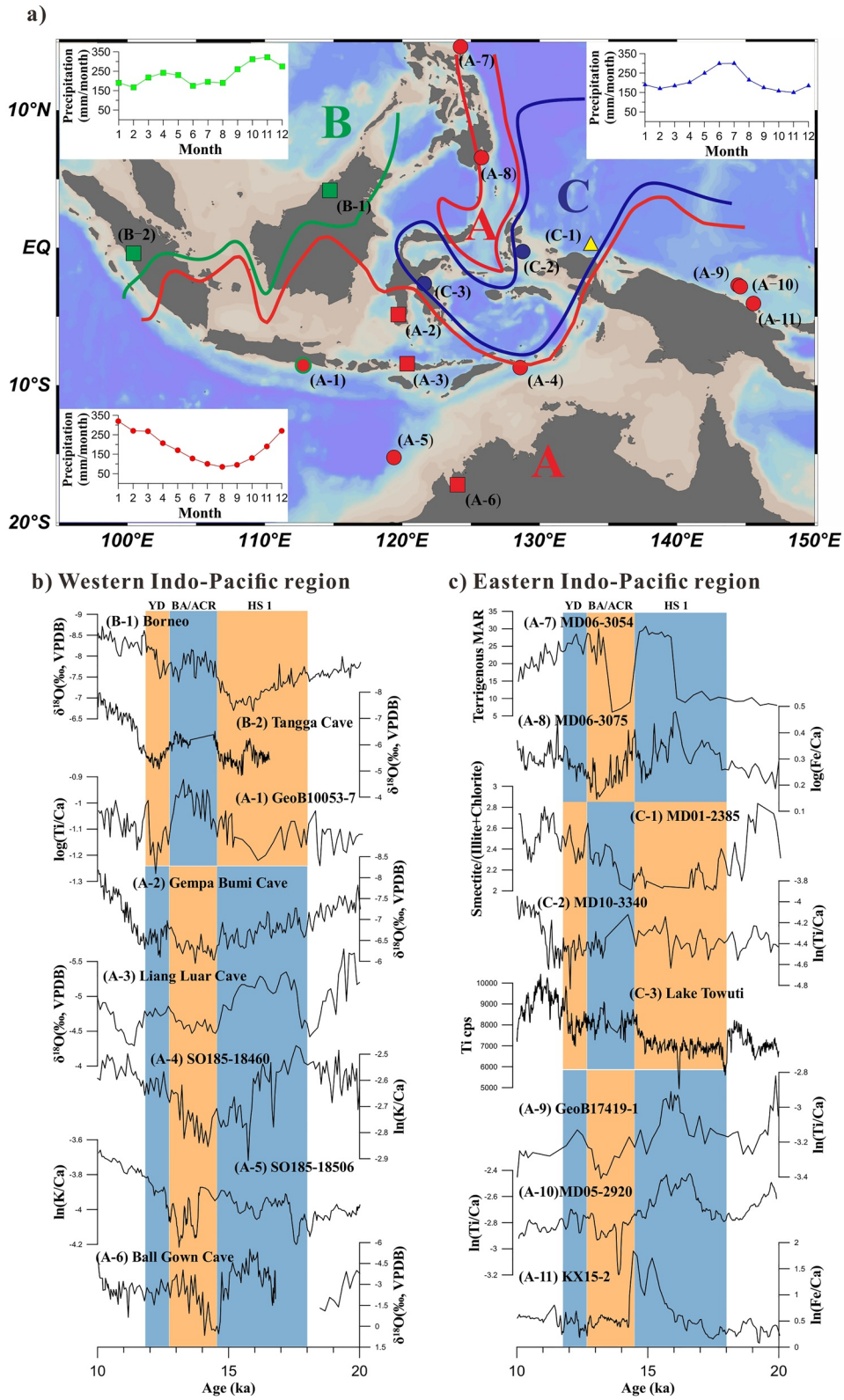

Figure 1.

In detail, three climatic regions can be identified in the Indo-Pacific region (Figure 1a), with distinct characteristics, based on monthly rainfall data from meteorological stations spanning 1961–1993 in the Global Historical Climatology Network database (Aldrian & Susanto, 2003). The potential source area supplying sediments to core MD01-2385 is the northwestern part of New Guinea, which is mostly located in region C. This region has higher precipitation in boreal summer and lower precipitation in boreal winter (Aldrian & Susanto, 2003) (Figure 1a). In contrast, the reverse precipitation pattern is observed in region A, with the highest precipitation of ∼320 mm/month in December–January (Figure 1a). Meanwhile, region B shows biannual precipitation peaks (∼310 mm/month in October–November and ∼250 mm/month in March–May) associated with the southward and northward movement of the ITCZ (Aldrian & Susanto, 2003). The geographic intrusion of region C with areas to both the west and east belonging to region A (Figure 1a) may arise from the westwards flow of the Indonesian Throughflow (Aldrian & Susanto, 2003). This current transports warm water from the Pacific warm pool, thereby generating an atmospheric convection center and bringing precipitation to the region during boreal summer, while the opposite scenario occurs during boreal winter (Aldrian & Susanto, 2003).

The island of New Guinea has very high riverine sediment fluxes (1,200 Mt/yr) and physical erosion rates (1,500 t/km^2/yr), reflecting its active tectonics, relatively young and easily weatherable basaltic rocks, and a tropical climate with heavy precipitation and runoff (Milliman & Farnsworth, 2013) (Figure S2 in Supporting Information S1). In addition, its small mountainous river catchments, with large elevation differences, small watershed areas, and short transport distances, lead to rapid and efficient sediment transfer to the oceans (Milliman & Farnsworth, 2013) (Figure S2 in Supporting Information S1).

3. Results

The clay mineral assemblage in core MD01-2385 consists predominantly of smectite (28%–86%, average 67%), while illite (5%–49%, average 17%), chlorite (5%–28%, average 14%), and kaolinite (0.5%–8%, average 2%) are less abundant (see Materials and Methods in Supporting Information S1; Figure S3 in Supporting Information S1). Variations in smectite content are opposite to those of illite and chlorite, and the smectite/(illite + chlorite) ratio is used as an indicator of clay composition variations. Relatively high smectite/(illite + chlorite) ratios appear during glacial intervals from 40 to 27 ka and during the early to middle Holocene from 12 to 5 ka (Figure 2a and Figure S3 in Supporting Information S1). In contrast, lower values characterize the LGM and the last deglaciation from 27 to 12 ka and the late Holocene from 5 to 0 ka. Notably, the smectite/(illite + chlorite) ratio decreased during the late Holocene from 5 to 0 ka, and reached its lowest absolute values (lower even than during the LGM) in the youngest sediments (Figure 2a and Figure S3 in Supporting Information S1). Another important observation is that the smectite/(illite + chlorite) ratios persistently co-vary with the zonal Pacific ΔSST anomaly, with generally lower values in both records during the North Atlantic cold events of HS 1–4 and during some other muti-millennial intervals (Figures 2a and 2b).

The Chemical Index of Alteration (CIA) in the clay-sized fraction in core MD01-2385 ranges from 74 to 78 (see Materials and Methods in Supporting Information S1; Figure 2c), which appears to indicate some temporal variability in the chemical weathering intensity. Another useful tracer in this regard is the Rb/Sr ratio, because Rb is enriched in the fine fractions, while Sr is highly mobile during chemical weathering (Chang et al., 2013). Hence, the Rb/Sr ratio can reflect the intensity of chemical weathering, with higher Rb/Sr ratios indicating higher chemical weathering degree (Chang et al., 2013). The Rb/Sr ratios in core MD01-2385 range from 0.65 to 0.95 (see

Figure 1. Comparison of modern and deglacial precipitation patterns in the Indo-Pacific region. (a) Map showing three regions (A, B, and C) with distinct precipitation patterns (inset figures), based on monthly rainfall data from meteorological stations spanning 1961–1993 in the Global Historical Climatology Network database (Aldrian & Susanto, 2003). Locations of millennial-scale paleoclimate reconstructions from each region are marked by symbols (circles, marine cores; squares, stalagmites; triangle, this study) and colored/labeled by region: (A-1) GeoB10053-7 (Mohtadi et al., 2011), (A-2) Gempa Bumi Cave (Krause et al., 2019), (A-3) Liang Luar Cave (Ayliffe et al., 2013; Griffiths et al., 2009), (A-4) SO185-18460 (Kuhnt et al., 2015), (A-5) SO185-18506 (Kuhnt et al., 2015), (A-6) Ball Gown Cave (Denniston et al., 2013), (A-7) MD06-3054 (Xiong et al., 2018), (A-8) MD06-3075 (Fraser et al., 2014), (A-9) GeoB17419-1 (Hollstein et al., 2018), (A-10) MD05-2920 (Tachikawa et al., 2011) and (A-11) KX15-2 (Dang, Wu, et al., 2020) from region A (red); (B-1) Borneo stalagmite (Carolin et al., 2013, 2016; Partin et al., 2007) and (B-2) Tangga Cave (Wurtzel et al., 2018) from region B (green); and (C-1) MD01-2385 (9-point running mean, this study; note that only the clay mineralogy proxy is shown here), (C-2) MD10-3340 (Dang et al., 2015), and (C-3) Lake Towuti (Russell et al., 2014) from region C (blue). (b) Deglacial precipitation reconstructions in the western Indo-Pacific region (i.e., eastern Indian Ocean). Note that (A-1) GeoB10053-7 is located in region A, but shows decreasing precipitation during the Younger Dryas and HS 1, similar to region B records. (c) Deglacial precipitation reconstructions in the eastern Indo-Pacific region (i.e., western Pacific Ocean). All records are plotted such that upwards indicates increased precipitation, and are presented on their original published age models. Blue/orange shading indicates higher/lower precipitation, respectively. HS 1, Heinrich Stadial 1; BA, Bølling–Allerød; ACR, Antarctic Cold Reversal; YD, Younger Dryas; MAR, Mass Accumulation Rate.

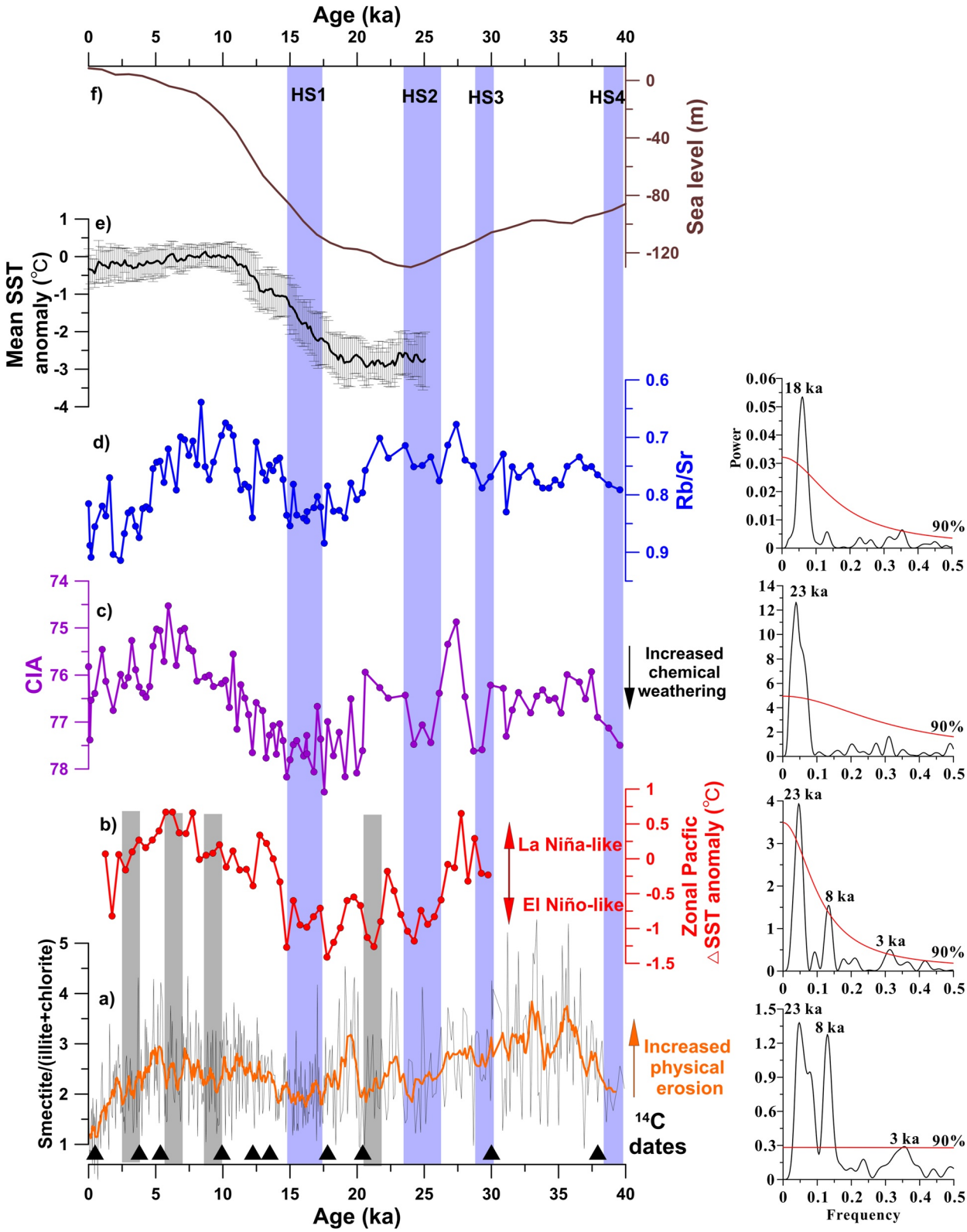

Figure 2.

Materials and Methods in Supporting Information S1; Figure 2d). Both the CIA and Rb/Sr ratios display similar long-term variations to the record of smectite/(illite + chlorite) ratios, with lower CIA and Rb/Sr ratios generally corresponding to higher smectite/(illite + chlorite) ratios (note the inverse scales for CIA and Rb/Sr ratios on Figure 2). This co-variation is also seen during the millennial-scale events of HS 1–4, with increased CIA and Rb/Sr ratios accompanying the lower smectite/(illite + chlorite) ratios (Figure 2). However, while noting the relatively lower resolution of these chemical records, we also recognize some discrepancies with the clay mineral record on multi-millennial timescales. For example, outside of the HS 1–4 events, no clear multi-millennial variation is observed in the CIA or Rb/Sr records. In addition, spectral analysis demonstrates that all of the records contain a strong precession periodicity (Figures 2a–2d), whereas only the smectite/(illite + chlorite) record and the zonal Pacific ΔSST anomaly show consistent multi-millennial periodicities at ∼8 and ∼3 ka (Figures 2a and 2b).

4. Discussion

4.1. Physical Erosion and Chemical Weathering Records From Core MD01-2385

Given its proximal location, the most important sediment source to core MD01-2385 is the island of New Guinea (Figure S2 in Supporting Information S1), with its northern slope and surrounding islands mainly comprising basic to intermediate volcanic rocks and their derived sediments (Wu et al., 2012). The high smectite content in core MD01-2385 (Figure S3 in Supporting Information S1) is consistent with rapid weathering of basaltic rocks in a wet and humid region (Wu et al., 2012). This inference is also supported by a similar dominance of smectite in the clay mineral assemblages of nearby KX cores from the northern margin of New Guinea (Dang, Wu, et al., 2020; Wu et al., 2012) (Figure S2 in Supporting Information S1). The above observations lead us to suggest that local sources in northwest New Guinea, in particular the northern margin of Bird's Head Peninsula, supplied most of the smectite to the study site via transport in small mountainous river systems (Figure S2 in Supporting Information S1).

The smectite/(illite + chlorite) ratios show fluctuations corresponding to both HS 1–4 and to the high-frequency multi-millennial ENSO-like variability (Figures 2a and 2b), whereas the geochemical ratios (CIA, Rb/Sr ratios) seem to record only the HS 1–4 events (Figures 2c and 2d). Furthermore, these proxies are anti-correlated, with elevated smectite/(illite + chlorite) ratios corresponding to lower CIA and Rb/Sr ratios. Such observations could be explained by a weathering regime in northwest New Guinea that is strongly controlled by physical erosion induced by heavy rainfall. In such a highly erosional regime, increases in precipitation can be expected to enhance both physical erosion rates and sediment transport efficiency in the drainage basins of New Guinea, leading to less time for sediments to be strongly chemically weathered in soils and hence driving the delivery of detrital minerals characterized by a lower degree of chemical weathering (i.e., lower CIA and Rb/Sr). In other words, while physical erosion rates and chemical weathering fluxes were both enhanced during wet conditions, the chemical weathering fluxes increased by proportionally less than the erosion rates, such that the degree of weathering of those sediments decreased (West, 2012). As a corollary, drier conditions, such as during HS 1–4, would lead to weaker runoff and reduced physical erosion rates, but a higher degree of chemical weathering of the detrital minerals due to their longer residence times in soils. Given that the basalt-dominated lithology and hot, humid climate favor the production and supply of smectite by physical erosion, the variations of illite and chlorite are considered to represent background sedimentation, while changes in smectite/(illite + chlorite) ratios are related to physical erosion-controlled variations in smectite input.

Figure 2. Comparison of millennial-scale weathering and climate records. (a) Smectite/(illite + chlorite) ratios in core MD01-2385, interpreted as an erosion indicator (this study). Black lines are individual data points and orange lines are 9-point running mean. The black triangles represent calibrated ^{14}C ages. (b) Variations in the ENSO-like system, indicated by the zonal Pacific ΔSST anomaly from a compilation of sea surface temperature (SST) data (Koutavas & Joanides, 2012). (c) Chemical weathering intensity in core MD01-2385 (this study) based on the chemical index of alteration CIA = $(Al_2O_3/(Al_2O_3 + CaO^* + Na_2O + K_2O)) \times 100$, where CaO* represents CaO associated with the silicate fraction (Nesbitt & Young, 1982). (d) Rb/Sr ratio in core MD01-2385 (this study). Note that the *y*-axes of panels (c) and (d) are reversed. (e) Stacked SST anomaly relative to the mean of each record from 6 to 10 ka for the Indo-Pacific Warm Pool (Dang, Jian, et al., 2020). Error bars represent 2SD. (f) Global sea-level reconstruction (Spratt & Lisiecki, 2016). North Atlantic cold events of Heinrich Stadials (HS) 1–4 and other multi-millennial intervals are labeled and indicated with blue and gray bars, respectively. Spectral analysis of each record (a–d) is shown on the right, calculated using the PAST software. Red lines are 90% confidence levels.

4.2. Reconstruction of Precipitation Changes in Northwestern New Guinea

The main climatic factors affecting the terrigenous weathering of a given region during the Late Quaternary are precipitation and temperature (Chamley, 1989; West et al., 2005). In the IPWP region, tropical SST anomalies do not reveal significant variability during the North Atlantic cold events (Dang, Jian, et al., 2020; Koutavas & Joanides, 2012) (Figure 2e), and this muted tropical temperature variability over millennial timescales is widely supported in numerous studies (Chiang, 2009; Graham & Barnett, 1987; Shakun et al., 2012). Therefore, we suggest that the millennial-scale variations in the weathering and erosion records in core MD01-2385 must have been mainly influenced by precipitation (rather than temperature), and so can be used as an indicator of tropical precipitation changes. Such an interpretation is also consistent with a study of clay mineralogy in the nearby KX cores (Figure S2 in Supporting Information S1), which proposed that precipitation was the main controlling factor on regional weathering (Wu et al., 2012).

Given that core MD01-2385 is located in the center of the IPWP region, the precipitation intensity inferred from our weathering and erosion records is expected to reflect changes in the intensity of the deep atmospheric convection center in the IPWP and/or spatial migration of the convection center. Therefore, the modern relationship between the zonal Pacific SST gradient, ENSO variability, and IPWP precipitation can be invoked to explain the similar millennial-scale variations (Koutavas & Joanides, 2012) (Figures 2a–2d). Specifically, negative zonal Pacific ΔSST anomalies generally correspond to lower smectite/(illite + chlorite) ratios during HS 1–3 and other high-frequency multi-millennial intervals throughout the record (Figures 2a and 2b). This pattern could be explained by frequent El Niño-like conditions leading to a weakened Walker circulation and an eastward-shifted precipitation center. In contrast, positive zonal Pacific ΔSST anomalies indicate La Niña-like conditions and an enhanced Walker circulation during both warm interstadial events and the early to middle Holocene, which could strengthen precipitation in northwest New Guinea (Figures 2a and 2b). The different responses of smectite/(illite + chlorite) ratios and geochemical indicators (CIA, Rb/Sr ratios) to the high-frequency ENSO-like variability (Figures 2a–2d) could be related to a different sensitivity of physical erosion and chemical weathering processes in response to precipitation changes. For example, the HS events may have involved more extreme and/or longer-lasting precipitation changes that affected both the weathering and erosion indicators, whereas only the erosion indicators show a clear response to the shorter and/or weaker perturbations corresponding to ENSO-like variability outside of HS events.

The decrease in smectite/(illite + chlorite) ratios (Figure 2a) and the corresponding increase in Rb/Sr ratios during the late Holocene (Figure 2d) are also consistent with a trend toward more negative zonal Pacific ΔSST anomalies (Figure 2d), which suggests a weakening of the Walker circulation toward the present-day that would lead to reduced precipitation in this region. Such a late Holocene weakening of the Walker circulation is in agreement with coupled climate model experiments (DiNezio et al., 2011) and with proxies for thermocline depth and rainfall in the eastern tropical Indian Ocean (Mohtadi et al., 2017). The proxy records from the latter study also suggested that the Walker circulation was weaker during the late Holocene than during the LGM (Mohtadi et al., 2017), which is supported by the lower smectite/(illite + chlorite) ratios and higher Rb/Sr ratios observed for the late Holocene than the LGM in core MD01-2385. However, a stronger-than-modern Walker circulation during the LGM is in conflict with a synthesis of proxy reconstructions and a multi-model ensemble of climate simulations (Liu et al., 2009), which could point to inconsistent variations of the Walker circulation intensity in different regions.

4.3. Spatial Patterns of Millennial-Scale Precipitation Changes in the Indo-Pacific Region

Comparing our new record to existing records from the Indo-Pacific region provides a better understanding of the mechanisms controlling precipitation variability on millennial timescales. In core MD01-2385 (C-1, Figure 1a), the lower smectite/(illite + chlorite) ratios during HS 1 imply decreased precipitation, which is inconsistent with the increased precipitation at this time inferred from several nearby cores in the eastern Indo-Pacific region (A-7 and A-8 in the north, and A-9 to A-11 in the south; Figures 1a and 1c), indicating a complex spatial pattern of precipitation variability. These sites are located within different hydrological regimes in the modern day (i.e., zones A and C; Figure 1), which may help to explain the heterogeneous precipitation patterns on millennial timescales.

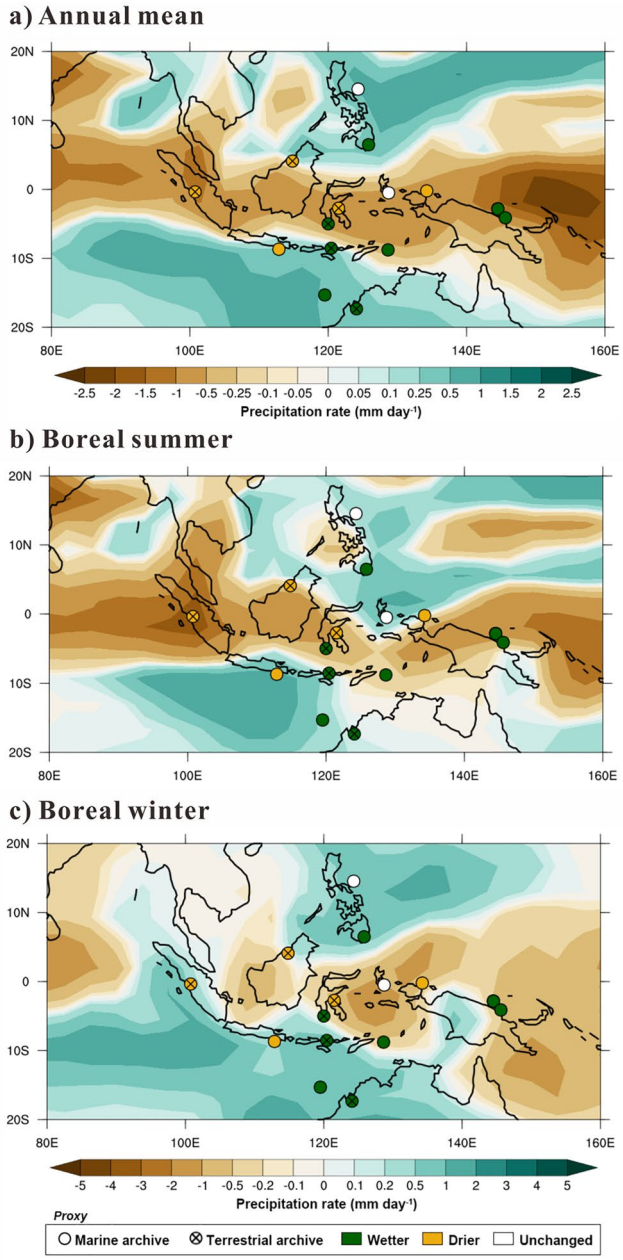

Figure 3. Comparison of precipitation anomalies for HS 1 minus the Bølling–Allerød (BA) for TraCE-21 modeling results (color shading) (Liu et al., 2009) and the paleo-proxies (symbols) for (a) the annual mean, (b) boreal summer, and (c) boreal winter. For details of the paleo-proxy records, see Figure 1. The average values from each of the two intervals (BA: 14.7−13 ka; HS 1: 17−15 ka) were used. The significance of the difference between HS 1 and the BA in each proxy record was tested using a Student's *t*-test and the p values are provided in Supporting Information S1 (Table S1).

To explore the drivers of such millennial-scale precipitation heterogeneity in the Indo-Pacific region, precipitation values of HS1 minus BA were calculated from both the modeling results of TraCE-21 and the new compiled paleo-proxy records (Table S1 in Supporting Information S1), and then put together for comparison (see Materials and Methods in Supporting Information S1; Figure 3 and Table S1 in Supporting Information S1). The paleo-reconstructions are generally in broad agreement with the modeling results when the annual mean precipitation is considered (Figure 3a). In the modeling results for boreal summer, the western Indo-Pacific region (Indian Ocean) shows a "meridional" structure reflecting the ITCZ migration (Figure 3b), while the modeling results for boreal winter reveal a "sandwich" structure in the eastern part (western Pacific Ocean) (Figure 3c). The "sandwich" structure is characterized by weaker precipitation over regions including Sulawesi, and the Banda Sea, sandwiched by regions with higher precipitation including the Luzon Islands, central New Guinea, and northern Australia. Such a "sandwich" structure could not be explained simply by ITCZ migration, and calls for additional influences.

During the last deglaciation, sea-level rise also had the potential to affect the intensity of the Walker circulation and the regional precipitation by changing the land-sea configuration (DiNezio & Tierney, 2013). Additionally, rising sea level could potentially have affected certain precipitation proxies at specific sites, by providing a more proximal moisture source, and a more distal position of marine cores relative to the terrestrial shoreline (Konecky et al., 2016) (Figure 2f). However, any sea-level effect on the proxies in the cores located in the eastern Indo-Pacific region was unlikely to be pronounced, given the narrow continental shelves on the eastern margins of Luzon and New Guinea islands and the lack of variability in millennial-scale palaeo-coastline reconstructions from this region (Hanebuth et al., 2011). This inference is also supported by the fact that the gradual deglacial sea-level rise (Figure 2f) could potentially explain either a gradual shift or a jump in a proxy record due to a threshold effect, but should not cause fluctuations back and forth, such as those observed (Figures 1b and 1c).

To further investigate the potential factors affecting the precipitation changes in the IPWP, we additionally considered single-forcing experiments in the TraCE-21 modeling (Figure S4 in Supporting Information S1). We found that both the "meridional" structure in the western part and the "sandwich" structure in the eastern part are most significant in the meltwater fluxes (MWF) experiment rather than in the orbital parameters (ORB) or greenhouse gas concentrations (GHG) experiments (Figure S4 in Supporting Information S1). In the ice volume experiment (ICE), precipitation changes are weaker than in the other experiments, and a "sandwich" structure rather than a "meridional" one is simulated in the western part. Therefore, these experiments further support that a sea-level effect is probably not a significant driver of the millennial-scale precipitation changes recorded by our record. Instead, meltwater forcing appears to have been an important driver of the millennial-scale precipitation variability, since this forcing on its own produces a fairly good fit to the data (Figure S4 in Supporting Information S1).

The "meridional" structure in the western Indo-Pacific region (Indian Ocean) describes two regions that are separated by the mean position of the ITCZ (Figure 3), which can be expected to vary through time in response to interhemispheric temperature asymmetry. In contrast, a clear "sandwich" structure is seen in the eastern Indo-Pacific region (Western Pacific) (Figure 3), which is more significant in winter in the meltwater flux (MWF) experiment (Figure S4 in Supporting Information S1). Such a modeling result may be related to the ENSO-like conditions and Pacific Walker circulation that

would have shifted the precipitation center in and/or away from the western Indo-Pacific region. This hypothesis is supported by the consistent variations between the zonal Pacific ΔSST anomaly and our weathering and erosion records, particularly the smectite/(illite + chlorite) ratios (Figure 2). Since the ITCZ and ENSO systems have higher frequency cycles than those resolved here, we also speculate that this complex precipitation pattern in the IPWP may not only be present on millennial timescales, but also on shorter timescales, although future studies would be needed to verify such a hypothesis.

5. Conclusions

High-resolution records of clay mineralogy and elemental chemistry in sediment core MD01-2385 from the IPWP were used to reconstruct sub-millennial precipitation changes within the IPWP over the last 40,000 years. These weathering and erosion records are used as precipitation proxies and are interpreted in terms of changes in the intensity or migration of deep convection in the IPWP. We found that higher smectite/(illite + chlorite) ratios and lower CIA and Rb/Sr ratios coincided with strong zonal Pacific ΔSST anomalies during North Atlantic warm interstadials and the early to middle Holocene, which suggests that a La Niña-like state and strong Walker circulation strengthened the regional precipitation. In contrast, lower smectite/(illite + chlorite) ratios and higher CIA and Rb/Sr ratios were coincident with weak zonal Pacific ΔSST anomalies during North Atlantic cold HS events and the late Holocene, implying an El Niño-like state and weak Walker circulation. In combination with a compilation of existing records and TraCE-21 modeling results, we demonstrate a spatially heterogeneous pattern of millennial-scale precipitation in the Indo-Pacific region, with the eastern part (West Pacific) mainly influenced by the ENSO-like system and the western part (Indian Ocean) mainly controlled by migration of the ITCZ. These results could provide a useful framework for future projections of atmospheric patterns and precipitation change in this region, although the behavior of this system under significantly warmer conditions than the pre-industrial climate was not tested here.

Data Availability Statement

The data are available at Zenodo (https://zenodo.org/record/7089974#.YybRP-mj5l8) and also in Supporting Information S1.

Acknowledgments
We thank the IPEV (Institut Polaire Emile Victor), the crews, and the scientific teams of the IMAGES VII Cruise 2001 for their excellent work during core sampling. We also thank Mahyar Mohtadi, two anonymous reviewers, and the editor for their very helpful comments on earlier versions of the manuscript. This study was supported by the Strategic Priority Research Program of Chinese Academy of Sciences (XDB42010402), the National Natural Science Foundation of China (91958107), Natural Science Foundation of Shandong (ZR2022YQ33), Youth Innovation Promotion Association, CAS (2020210), Laboratory for Marine Geology, Qingdao Pilot National Laboratory for Marine Science and Technology (MGQNLM-TD201902), Open Fund of the State Key Laboratory of Marine Geology, Tongji University (MGK1919). DJW was supported by a Natural Environment Research Council independent research fellowship (NE/T011440/1). For the purpose of open access, the author has applied a Creative Commons Attribution (CC BY) license to any Author Accepted Manuscript version arising.

References

Aldrian, E., & Susanto, R. (2003). Identification of three dominant rainfall regions within Indonesia and their relationship to sea surface temperature. *International Journal of Climatology: A Journal of the Royal Meteorological Society*, *23*(12), 1435–1452. https://doi.org/10.1002/joc.950

Ayliffe, L. K., Gagan, M. K., Zhao, J. X., Drysdale, R. N., Hellstrom, J. C., Hantoro, W. S., et al. (2013). Rapid interhemispheric climate links via the Australasian monsoon during the last deglaciation. *Nature Communications*, *4*(1), 2908. https://doi.org/10.1038/ncomms3908

Carolin, S. A., Cobb, K. M., Adkins, J. F., Clark, B., Conroy, J. L., Lejau, S., et al. (2013). Varied response of western Pacific hydrology to climate forcings over the last glacial period. *Science*, *340*(6140), 1564–1566. https://doi.org/10.1126/science.1233797

Carolin, S. A., Cobb, K. M., Lynch-Stieglitz, J., Moerman, J. W., Partin, J. W., Lejau, S., et al. (2016). Northern Borneo stalagmite records reveal West Pacific hydroclimate across MIS 5 and 6. *Earth and Planetary Science Letters*, *439*, 182–193. https://doi.org/10.1016/j.epsl.2016.01.028

Chamley. (1989). *Clay sedimentology*. Springer.

Chang, H., An, Z., Wu, F., Jin, Z., Liu, W., & Song, Y. (2013). A Rb/Sr record of the weathering response to environmental changes in westerly winds across the Tarim Basin in the late Miocene to the early Pleistocene. *Palaeogeography, Palaeoclimatology, Palaeoecology*, *386*, 364–373. https://doi.org/10.1016/j.palaeo.2013.06.006

Chiang, J. C. H. (2009). The tropics in paleoclimate. *Annual Review of Earth and Planetary Sciences*, *37*(37), 263–297. https://doi.org/10.1146/annurev.earth.031208.100217

Dang, H., Jian, Z., Kissel, C., & Bassinot, F. (2015). Precessional changes in the western equatorial Pacific hydroclimate: A 240 Kyr marine record from the Halmahera Sea, East Indonesia. *Geochemistry, Geophysics, Geosystems*, *16*(1), 148–164. https://doi.org/10.1002/2014gc005550

Dang, H., Jian, Z., Wang, Y., Mohtadi, M., Rosenthal, Y., Ye, L., et al. (2020). Pacific warm pool subsurface heat sequestration modulated Walker circulation and ENSO activity during the Holocene. *Science Advances*, *6*(42), eabc0402. https://doi.org/10.1126/sciadv.abc0402

Dang, H., Wu, J., Xiong, Z., Qiao, P., Li, T., & Jian, Z. (2020). Orbital and sea-level changes regulate the iron-associated sediment supplies from Papua New Guinea to the equatorial Pacific. *Quaternary Science Reviews*, *239*, 106361. https://doi.org/10.1016/j.quascirev.2020.106361

Denniston, R. F., Wyrwoll, K.-H., Asmerom, Y., Polyak, V. J., Humphreys, W. F., Cugley, J., et al. (2013). North Atlantic forcing of millennial-scale Indo-Australian monsoon dynamics during the Last Glacial period. *Quaternary Science Reviews*, *72*, 159–168. https://doi.org/10.1016/j.quascirev.2013.04.012

DiNezio, P. N., Clement, A., Vecchi, G. A., Soden, B., Broccoli, A. J., Otto-Bliesner, B. L., & Braconnot, P. (2011). The response of the Walker circulation to Last Glacial Maximum forcing: Implications for detection in proxies. *Paleoceanography*, *26*(3). https://doi.org/10.1029/2010pa002083

DiNezio, P. N., & Tierney, J. E. (2013). The effect of sea level on glacial Indo-Pacific climate. *Nature Geoscience*, *6*(6), 485–491. https://doi.org/10.1038/ngeo1823

Fraser, N., Kuhnt, W., Holbourn, A., Bolliet, T., Andersen, N., Blanz, T., & Beaufort, L. (2014). Precipitation variability within the West Pacific warm pool over the past 120 ka: Evidence from the Davao Gulf, southern Philippines. *Paleoceanography*, *29*(11), 1094–1110. https://doi.org/10.1002/2013pa002599

Graham, N., & Barnett, T. (1987). Sea surface temperature, surface wind divergence, and convection over tropical oceans. *Science*, *238*(4827), 657–659. https://doi.org/10.1126/science.238.4827.657

Griffiths, M. L., Drysdale, R. N., Gagan, M. K., Zhao, J. X., Ayliffe, L. K., Hellstrom, J. C., et al. (2009). Increasing Australian–Indonesian monsoon rainfall linked to early Holocene sea-level rise. *Nature Geoscience*, *2*(9), 636–639. https://doi.org/10.1038/ngeo605

Hanebuth, T. J., Voris, H. K., Yokoyama, Y., Saito, Y., & Okuno, J. I. (2011). Formation and fate of sedimentary depocentres on Southeast Asia's Sunda Shelf over the past sea-level cycle and biogeographic implications. *Earth-Science Reviews*, *104*(1–3), 92–110. https://doi.org/10.1016/j.earscirev.2010.09.006

Hollstein, M., Mohtadi, M., Rosenthal, Y., Prange, M., Oppo, D. W., Méndez, G. M., et al. (2018). Variations in Western Pacific Warm Pool surface and thermocline conditions over the past 110, 000 years: Forcing mechanisms and implications for the glacial Walker circulation. *Quaternary Science Reviews*, *201*, 429–445. https://doi.org/10.1016/j.quascirev.2018.10.030

Huang, Y., Xiao, J., Xiang, R., Liu, S., Khokiattiwong, S., Kornkanitnan, N., et al. (2020). Holocene Indian Summer Monsoon variations inferred from end-member modeling of sediment grain size in the Andaman Sea. *Quaternary International*, *558*, 28–38. https://doi.org/10.1016/j.quaint.2020.08.032

Konecky, B., Russell, J., & Bijaksana, S. (2016). Glacial aridity in central Indonesia coeval with intensified monsoon circulation. *Earth and Planetary Science Letters*, *437*, 15–24. https://doi.org/10.1016/j.epsl.2015.12.037

Koutavas, A., & Joanides, S. (2012). El Niño–Southern Oscillation extrema in the Holocene and Last Glacial Maximum. *Paleoceanography*, *27*(4). https://doi.org/10.1029/2012pa002378

Krause, C. E., Gagan, M. K., Dunbar, G. B., Hantoro, W. S., Hellstrom, J. C., Cheng, H., et al. (2019). Spatio-temporal evolution of Australasian monsoon hydroclimate over the last 40, 000 years. *Earth and Planetary Science Letters*, *513*, 103–112. https://doi.org/10.1016/j.epsl.2019.01.045

Kuhnt, W., Holbourn, A., Xu, J., Opdyke, B., De Deckker, P., Röhl, U., & Mudelsee, M. (2015). Southern Hemisphere control on Australian monsoon variability during the late deglaciation and Holocene. *Nature Communications*, *6*(1), 1–7. https://doi.org/10.1038/ncomms6916

Leduc, G., Vidal, L., Tachikawa, K., & Bard, E. (2009). ITCZ rather than ENSO signature for abrupt climate changes across the tropical Pacific? *Quaternary Research*, *72*(1), 123–131. https://doi.org/10.1016/j.yqres.2009.03.006

Liu, Z., Lu, Z., Wen, X., Otto-Bliesner, B. L., Timmermann, A., & Cobb, K. M. (2014). Evolution and forcing mechanisms of El Nino over the past 21, 000 years. *Nature*, *515*(7528), 550–553. https://doi.org/10.1038/nature13963

Liu, Z., Otto-Bliesner, B., He, F., Brady, E., Tomas, R., Clark, P., et al. (2009). Transient simulation of last deglaciation with a new mechanism for Bølling-Allerød warming. *Science*, *325*(5938), 310–314. https://doi.org/10.1126/science.1171041

Milliman, J. D., & Farnsworth, K. L. (2013). *River discharge to the coastal ocean: A global synthesis*. Cambridge University Press.

Mohtadi, M., Oppo, D. W., Steinke, S., Stuut, J.-B. W., De Pol-Holz, R., Hebbeln, D., & Lückge, A. (2011). Glacial to Holocene swings of the Australian–Indonesian monsoon. *Nature Geoscience*, *4*(8), 540–544. https://doi.org/10.1038/ngeo1209

Mohtadi, M., Prange, M., Oppo, D. W., De Pol-Holz, R., Merkel, U., Zhang, X., et al. (2014). North Atlantic forcing of tropical Indian Ocean climate. *Nature*, *509*(7498), 76–80. https://doi.org/10.1038/nature13196

Mohtadi, M., Prange, M., Schefuß, E., & Jennerjahn, T. C. (2017). Late Holocene slowdown of the Indian ocean walker circulation. *Nature Communications*, *8*(1), 1–8. https://doi.org/10.1038/s41467-017-00855-3

Mohtadi, M., Prange, M., & Steinke, S. (2016). Palaeoclimatic insights into forcing and response of monsoon rainfall. *Nature*, *533*(7602), 191–199. https://doi.org/10.1038/nature17450

Nesbitt, H., & Young, G. (1982). Early Proterozoic climates and plate motions inferred from major element chemistry of lutites. *Nature*, *299*(5885), 715–717. https://doi.org/10.1038/299715a0

Partin, J. W., Cobb, K. M., Adkins, J. F., Clark, B., & Fernandez, D. P. (2007). Millennial-scale trends in west Pacific warm pool hydrology since the Last Glacial Maximum. *Nature*, *449*(7161), 452–455. https://doi.org/10.1038/nature06164

Russell, J. M., Vogel, H., Konecky, B. L., Bijaksana, S., Huang, Y., Melles, M., et al. (2014). Glacial forcing of central Indonesian hydroclimate since 60, 000 y BP. *Proceedings of the National Academy of Sciences of the United States of America*, *111*(14), 5100–5105. https://doi.org/10.1073/pnas.1402373111

Sardeshmukh, P. D., & Hoskins, B. J. (1988). The generation of global rotational flow by steady idealized tropical divergence. *Journal of the Atmospheric Sciences*, *45*(7), 1228–1251. https://doi.org/10.1175/1520-0469(1988)045<1228:tgogrf>2.0.co;2

Schneider, T., Bischoff, T., & Haug, G. H. (2014). Migrations and dynamics of the intertropical convergence zone. *Nature*, *513*(7516), 45–53. https://doi.org/10.1038/nature13636

Schröder, J. F., Kuhnt, W., Holbourn, A., Beil, S., Zhang, P., Hendrizan, M., & Xu, J. (2018). Deglacial warming and hydroclimate variability in the central Indonesian archipelago. *Paleoceanography and Paleoclimatology*, *33*(9), 974–993. https://doi.org/10.1029/2018pa003323

Shakun, J. D., Clark, P. U., He, F., Marcott, S. A., Mix, A. C., Liu, Z., et al. (2012). Global warming preceded by increasing carbon dioxide concentrations during the last deglaciation. *Nature*, *484*(7392), 49–54. https://doi.org/10.1038/nature10915

Spratt, R. M., & Lisiecki, L. E. (2016). A Late Pleistocene sea level stack. *Climate of the Past*, *12*(4), 1079–1092. https://doi.org/10.5194/cp-12-1079-2016

Tachikawa, K., Cartapanis, O., Vidal, L., Beaufort, L., Barlyaeva, T., & Bard, E. (2011). The precession phase of hydrological variability in the Western Pacific Warm Pool during the past 400 ka. *Quaternary Science Reviews*, *30*(25), 3716–3727. https://doi.org/10.1016/j.quascirev.2011.09.016

Timmermann, A., An, S. I., Krebs, U., & Goosse, H. (2005). ENSO suppression due to weakening of the North Atlantic thermohaline circulation. *Journal of Climate*, *18*(16), 3122–3139. https://doi.org/10.1175/jcli3495.1

Turney, C. S., Kershaw, A. P., Clemens, S. C., Branch, N., Moss, P. T., & Fifield, L. K. (2004). Millennial and orbital variations of El Nino/Southern Oscillation and high-latitude climate in the last glacial period. *Nature*, *428*(6980), 306–310. https://doi.org/10.1038/nature02386

West, A. J. (2012). Thickness of the chemical weathering zone and implications for erosional and climatic drivers of weathering and for carbon-cycle feedbacks. *Geology*, *40*(9), 811–814. https://doi.org/10.1130/g33041.1

West, A. J., Galy, A., & Bickle, M. (2005). Tectonic and climatic controls on silicate weathering. *Earth and Planetary Science Letters*, *235*(1), 211–228. https://doi.org/10.1016/j.epsl.2005.03.020

Wu, J., Liu, Z., & Zhou, C. (2012). Late quaternary glacial cycle and precessional period of clay mineral assemblages in the western Pacific warm pool. *Chinese Science Bulletin*, *57*(28), 3748–3760. https://doi.org/10.1007/s11434-012-5277-x

Wurtzel, J. B., Abram, N. J., Lewis, S. C., Bajo, P., Hellstrom, J. C., Troitzsch, U., & Heslop, D. (2018). Tropical Indo-Pacific hydroclimate response to North Atlantic forcing during the last deglaciation as recorded by a speleothem from Sumatra, Indonesia. *Earth and Planetary Science Letters*, *492*, 264–278. https://doi.org/10.1016/j.epsl.2018.04.001

Xiong, Z., Li, T., Chang, F., Algeo, T. J., Clift, P. D., Bretschneider, L., et al. (2018). Rapid precipitation changes in the tropical West Pacific linked to North Atlantic climate forcing during the last deglaciation. *Quaternary Science Reviews*, *197*, 288–306. https://doi.org/10.1016/j.quascirev.2018.07.040

Zhang, R., & Delworth, T. L. (2005). Simulated tropical response to a substantial weakening of the Atlantic thermohaline circulation. *Journal of Climate*, *18*(12), 1853–1860. https://doi.org/10.1175/jcli3460.1

References From the Supporting Information

Cao, F., Yang, S., Yang, C., Guo, Y., Bi, L., & Li, Y. (2021). Using lithium isotopes to quantitatively decode continental weathering signal: A case study in the Changjiang (Yangtze River) Estuary. *Science China Earth Sciences*, *64*(10), 1–11. https://doi.org/10.1007/s11430-021-9811-5

Collins, W. D., Bitz, C. M., Blackmon, M. L., Bonan, G. B., Bretherton, C. S., Carton, J. A., et al. (2006). The community climate system model version 3 (CCSM3). *Journal of Climate*, *19*(11), 2122–2143. https://doi.org/10.1175/jcli3761.1

Heaton, T. J., Köhler, P., Butzin, M., Bard, E., Reimer, R. W., Austin, W. E., et al. (2020). Marine20—The marine radiocarbon age calibration curve (0–55, 000 cal BP). *Radiocarbon*, *62*(4), 779–820. https://doi.org/10.1017/rdc.2020.68

Wan, S., Toucanne, S., Clift, P. D., Zhao, D., Bayon, G., Yu, Z., et al. (2015). Human impact overwhelms long-term climate control of weathering and erosion in southwest China. *Geology*, *43*(5), 439–442. https://doi.org/10.1130/g36570.1

Wan, S., Yu, Z., Clift, P. D., Sun, H., Li, A., & Li, T. (2012). History of Asian eolian input to the West Philippine Sea over the last one million years. *Palaeogeography, Palaeoclimatology, Palaeoecology*, *326*, 152–159. https://doi.org/10.1016/j.palaeo.2012.02.015

Wu, Q., Colin, C., Liu, Z., Bassinot, F., Dubois-Dauphin, Q., Douville, E., et al. (2017). Foraminiferal εNd in the deep north-western subtropical Pacific Ocean: Tracing changes in weathering input over the last 30, 000 years. *Chemical Geology*, *470*, 55–66. https://doi.org/10.1016/j.chemgeo.2017.08.022